

Interactive Object Segmentation in 3D Point Clouds

Theodora Kontogianni^{1,2}, Ekin Celikkan³,
Siyu Tang¹, and Konrad Schindler¹

¹ ETH, Zurich, Switzerland

² ETH AI Center, Zurich, Switzerland

³ RWTH Aachen University, Germany

Abstract. Deep learning depends on large amounts of labeled training data. Manual labeling is expensive and represents a bottleneck, especially for tasks such as segmentation, where labels must be assigned down to the level of individual points. That challenge is even more daunting for 3D data: 3D point clouds contain millions of points per scene, and their accurate annotation is markedly more time-consuming. The situation is further aggravated by the added complexity of user interfaces for 3D point clouds, which slows down annotation even more. For the case of 2D image segmentation, interactive techniques have become common, where user feedback in the form of a few clicks guides a segmentation algorithm – nowadays usually a neural network – to achieve an accurate labeling with minimal effort. Surprisingly, interactive segmentation of 3D scenes has not been explored much. Previous work has attempted to obtain accurate 3D segmentation masks using human feedback from the 2D domain, which is only possible if correctly aligned images are available together with the 3D point cloud, and it involves switching between the 2D and 3D domains. Here, we present an interactive 3D object segmentation method in which the user interacts directly with the 3D point cloud. Importantly, our model does not require training data from the target domain: when trained on ScanNet, it performs well on several other datasets with different data characteristics as well as different object classes. Moreover, our method is orthogonal to supervised (instance) segmentation methods and can be combined with them to refine automatic segmentations with minimal human effort.

1 Introduction

Just like other occurrences of supervised deep learning, 3D scene understanding tasks such as 3D semantic segmentation and instance segmentation require large amounts of annotated training data. Alas, dense manual annotation is an even more time-consuming and tedious effort in 3D. To obtain accurate 3D segmentation masks with as little human effort as possible, a natural idea is to adapt interactive object segmentation techniques, which are well-established for the 2D image domain, and commonly used to collect ground-truth segmentation masks at scale [4].

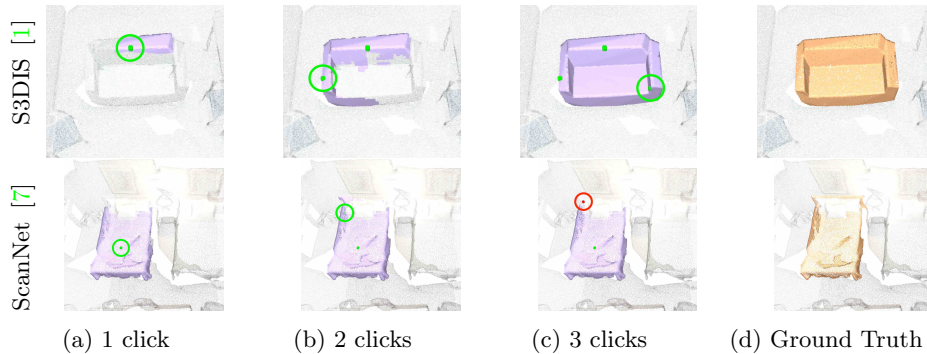


Fig. 1: **Interactive 3D Object Segmentation.** The model predicts a segmentation mask and iteratively updates it, driven by user feedback in the form of **positive** clicks on false negatives and **negative** clicks on false positives. Current click pointed out in enlarged circle.

The principle of interactive object segmentation [4, 16, 20, 22, 25, 33] is to let a user collaborate with a computational model when segmenting an object instance. By concentrating on one instance (eg., a specific chair) at a time, the task becomes a binary foreground/background segmentation. The segmentation mask is found with an iterative procedure: the model produces its best guess of a mask, then the user provides feedback in the form of corrections, which the model ingests to produce an updated mask. That sequence is repeated until the mask is deemed accurate enough. The corrections usually come in the form of clicks that identify locations with incorrect labels. *Negative* clicks identify false positives, where parts of the background are labeled as foreground. *Positive* clicks identify false negatives where parts of the object have been labeled as background.

Even though interactive segmentation in images is a well-established technology, and part of several consumer software products, little is known about its potential for labeling 3D point clouds. Despite the recent progress of 3D deep learning, and the persistent dearth of realistic large-scale training sets, interactive 3D object segmentation remains under-explored.

The field of 3D deep learning has witnessed significant progress in the past few years, particularly regarding semantic segmentation and instance segmentation in point clouds [14, 17, 24, 31, 34, 36]. Nonetheless, instance segmentation is not suitable for labeling new datasets. It requires lots of training data to begin with. More importantly, it cannot generalize to classes that were not part of the training set, a situation commonly encountered when labeling a new dataset. What is more, the resulting segmentations masks tend to have moderate accuracy ($<90\%$ IoU), which is impressive for an AI system, but not enough to serve as high-quality ground truth (see Fig. 4). Note, though, that our proposed interactive method is orthogonal to most instance segmentation algorithms and can be combined with them to obtain improved segmentation masks with little user input.

So far, there have been few attempts to make 3D object segmentation more efficient via user interaction [27, 37]. In these methods, user interaction takes place

in the 2D image domain, i.e., they additionally require images whose camera pose w.r.t. the point cloud is known, and associated 2D segmentation masks. In [27] the user interacts both with the 2D image and with the 3D point cloud (by dragging mesh vertices), forcing the user to switch between 2D and 3D views of the same object. Due to the transition between the 2D and 3D domains, both these methods employ custom network architectures, therefore their integration with existing standard backbones (like Minkovski Engine [6], KPconv [30], or Pointnet++ [26]) is not straight-forward.

Here, we propose an approach where the user interacts directly with the 3D point cloud. We argue that this direct approach has several advantages: *(i)* it obviates the need to supply images and their poses relative to the point cloud; *(ii)* it relieves the user of going back and forth between 2D and 3D interfaces; and *(iii)* it can be incorporated into any (point-based or voxel-based) 3D segmentation network. In our experiments, we use MinkowskiEngine [6], proven state-of-the-art architecture based on a sparse 3D voxel grid.

A user clicks in our system select a 3D point, around which we cut out a small cubic volume. The points within that volume serve as examples for false positives, respectively false negatives of the current network state, depending on whether they are assigned to the foreground or the background. Conveniently, this intuitive mode of interaction matches well with existing 3D labeling software that uses bounding boxes. Additionally, we have also created a rudimentary interface that allows the user to pick single 3D points.

A main motivation for interactive segmentation is the ability to train algorithms for new domains where no appropriate training sets are available. Our method supports this, as it is general and not tied to a specific scan pattern or class nomenclature. We train on single dataset, ScanNet [7], and evaluate on several others. In summary, we make the following contributions:

1. We set a first state of the art for interactive object segmentation purely using 3D point data, without additional images.
2. Study the simulation of user clicks for training purposes and introduce a practical policy to synthetically generate meaningful clicks.
3. We experimentally show that interactive 3D object segmentation can provide accurate instance masks across various datasets, with little human effort.
4. We show that the interactive 3D segmentation network generalises well to different (indoor) datasets.

The take-home message we hope to convey with this paper is that current 3D deep learning technology, in combination with a user in the loop, makes it possible to efficiently generate high-accuracy segmentations with limited training data. We hope that our work may spark further research into interactive segmentation of 3D scenes.

2 Related Work

Fully-Supervised 3D Instance Segmentation. Instance segmentation on point clouds is a fundamental task in 3D scene perception and it has been

thoroughly studied in the past few years [5, 9, 13, 18, 21, 32, 35]. Roughly the methods can be separated into two major categories: (1) *proposal-based* and (2) *clustering-based*. Proposal-based approaches [9, 13, 35] directly generate object proposals (inspired by Mask R-CNN [12] in 2D) and predict instance segmentation masks inside each proposal. Clustering-based learn per-point features in an embedding space and then use clustering methods to generate instance predictions [5, 18, 21, 32]. Although these methods have achieved remarkable results on existing datasets, they require large amounts of labeled data for training and cannot generalize to classes that are not part of the training set. Our proposed interactive method is orthogonal to most instance segmentation methods and can be combined with them to improve segmentation mask with little user input.

Weakly-Supervised learning on 3D point clouds. Compared to fully supervised methods, weakly supervised methods try to learn the task at hand with limited training examples or labels. Recently, several methods [14, 17, 24, 31, 34, 36] started to tackle 3D semantic segmentation in a weakly supervised manner aiming to achieve the performance of their fully supervised counterparts using fewer point labels to train neural networks. Hou et. al [15] proposed a method that uses contrastive learning to learn meaningful feature representations that can be fine-tuned with fewer labels. Liu et al. [24] proposed a self-training approach that uses a graph propagation module that iteratively propagates the sparse labels for semantic segmentation. Xu et al. [34] performed point cloud semantic segmentation by exploiting spatial and color smoothness constraints along with gradient approximation.

Although they achieve promising results, most of these works focus on semantic segmentation of 3D point clouds with limited labeled points and require additional post-processing steps to separate object instances. Additionally, they focus on achieving the performance of fully supervised methods with fewer labels and they do not specifically target high quality segmentation masks, necessary for creating new 3D datasets. Even though the weakly-supervised methods utilize fewer points they still need individually trained models for every dataset while interactive object segmentation provides masks for single object instances allowing fast instance annotation and uses a single trained model.

Interactive 3D Object Segmentation. There is limited work on interactive frameworks for annotating 3D objects. Shen et al. [27] propose a framework for interactive 3D object annotation using interaction both in the image and the 3d domain. At first, the user provides feedback about large errors with scribbles in 2D views of the 3D space. After that, the user corrects minor errors, by manipulating mesh vertices. The user needs to label the same object switching between two different modalities and that might be tiring for large scale labeling. Additionally the method requires a specialized architecture.

In contrast, we allow the user to label 3D points directly in 3D space and our method can be incorporated in any semantic or instance segmentation network for 3D point clouds. Its results shall improve when used with more powerful

architectures in the future.

3 Method

We start by formally defining the problem. Consider a 3D scene $P \in \mathcal{R}^{N \times C}$ where N is the number of 3D points in the scene and C the dimensionality of the features associated with each 3D point (if we only consider as features the xyz coordinates then $C = 3$).

In interactive 3D object segmentation, a model allows the user to segment the desired region in the scene by successively placing positive (*foreground*) or negative (*background*) feedback in the form of clicks on a 3D point. Every time a new click is placed, the model outputs a new updated segmentation. Once the user is satisfied with the mask of the intended object, the process concludes.

3.1 Input representation.

The input to the interactive object segmentation network consists of the 3D scene $P \in \mathcal{R}^{N \times C}$ where N the number of 3D points and C the number of input features (traditionally xyz) plus two additional channels T_p and T_n for the positive and negative clicks respectively. (see Fig. in supp.)

Click Encoding. To acquire an accurate segmentation mask for the object of interest, the user provides a sequence of positive and negative clicks. The positive clicks are considered on the object, and the negative clicks are on the background. These clicks are represented by their 3D coordinates in a 3D scene. S_p is a set of all positive user clicks, and S_n is the set of all negative ones. Benenson et al. [4] have done an extensive study on 2D clicks encodings and find that disks of a small radius outperform the other encodings (eg. distance transform) since their effects are more locally restricted [28]. For those reasons and to be compatible with user interfaces that support only bounding box selection we encode the clicks as cubes.

So we define the 2 additional channels T_p and T_n as follows:

$$T_p(p) = \begin{cases} 1, & \text{if } |x_p - x_q| \leq \text{edge} \text{ and } |y_p - y_q| \leq \text{edge} \text{ and } |z_p - z_q| \leq \text{edge} \\ 0, & \text{otherwise} \end{cases} \quad (1)$$

where $x_q \in S_p$ and edge the length of a cube edge (for an ablation study regarding the length of the cube edge please see Sec. 4). We define T_n for the negative clicks similarly with $x_q \in S_n$. See fig. So each user click channel has the same number of points as the 3D scene ($N \times 1$) with ones on all the 3D points inside a cube around the clicked point and zeros elsewhere. Then we concatenate the C channels of the 3D scene with T_p and T_n to compose a $N \times (C + 2)$ (3D scene, user interaction) input.

Simulating user clicks - Train. It is very expensive to collect clicks from real users that are enough to train deep neural networks. Therefore, we simulate

user clicks for training using random sampling as is common practice in the 2D domain [16, 20, 22, 25, 33]. We sample *positive* clicks uniformly at random on the target 3D object. *Negative* clicks are sampled uniformly at random from pixels around the object.

Simulating user clicks - Test. At test time, we add clicks one by one based on the errors of the currently predicted mask. We imitate a user who always clicks at the center of the region with the largest error. To obtain this error region, we need to compare all falsely labeled 3D points with all others. To reduce memory and computational requirements, we perform this operation on a voxelized version of the 3D scene, where we only consider the occupied voxels.

Online Adaptation. Interactive object segmentation can alleviate the issue of poor generalization on unknown classes and different datasets as seen in our results on different datasets (Table 3). Its generalization can be further improved (Table 3) by considering the user corrections as sparse training examples to update the model during test (labeling) time [19].

3.2 Network Architecture.

In this work, we adopt the Minkowski Engine [6] proposed by Choy et al., an extension of sparse convolutional networks [11]. Architectures based on the Minkowski Engine have shown impressive results on semantic segmentation. The sparse convolutions allow the efficient use of 3D convolutional layers and deep architectures already stapled in 2D vision.

All network weights except for the output layer are initialized with those provided by [6]. They were obtained by pretraining the network on the task of semantic segmentation on the ScanNetV2 dataset (Train) [7]. The input now has two additional channels for the user clicks, and the last output layer is replaced with a two-class softmax layer, which is used to produce binary segmentations (foreground/background). Finally the network is fine-tuned for the task of interactive object segmentation using the ScanNetV2 train dataset adapted for foreground/background segmentation: a ground truth segmentation mask is created for each object instance where a single object instance is labeled as foreground and every other point in the 3D scene as background. Ground-truth segmentation masks are created for all 3D instances in the ScanNetV2 train dataset. They are used to fine-tune the Minkowski Engine for the task of interactive object segmentation.

3.3 Implementation and Training Details

We set the input feature dimension $C = 6$ using position and color (without surface normals). For semanticKITTI [3] we use $C=3$ using only position. For the experiments on online adaptation we followed the protocol for instance adaptation (IS) from [19] using learning rate of $5 \cdot 10^{-5}$ and $\lambda = 0.1$. Further implementation details are provided in the supplementary material.

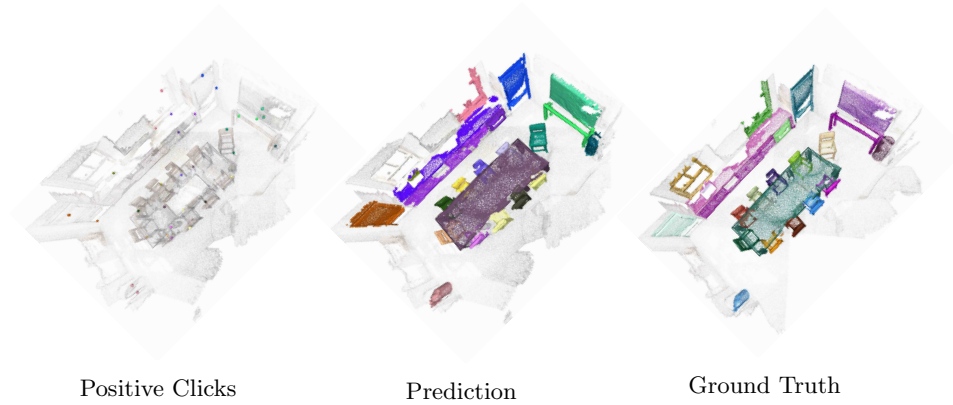


Fig. 3: **Example of 3D Instance Segmentation** using interactive object segmentation on a full 3D scene from ScanNetV2 [7] validation set. (*Left:*) Objects are annotated one by one, each color indicates a new instance (*Middle:*) Predictions obtained by the model given the user clicks. (*Right:*) Ground-Truth for reference, colors are picked at random so they do not necessarily match the prediction colors.

4 Experiments

4.1 Datasets

The interactive segmentation model (according to interactive object segmentation protocols from 2D) in all our experiments is pre-trained on a single dataset and tested on all others. In our work, we utilize the ScanNetV2 [7] train set since it is currently the largest of its kind containing approximately 1500 scenes. However, ScanNetV2 [7] is still much smaller in scale compared to the 2D datasets used in interactive object segmentation of 2D images. To compare, in 2D interactive object segmentation a typical deep learning model [25] is using the weights from pre-training on the ImageNet [8], COCO [23], and PASCAL VOC 2012 [10] datasets for the task of semantic segmentation and it is usually additionally fine-tuned on PASCAL VOC 2012 [10] for the task of interactive object segmentation.

We evaluate all the algorithms on three public datasets: ScanNetV2 [7] validation set, Stanford S3DIS [1] and SemanticKITTI [3].

ScanNetV2 train set. The ScanNetV2 [7] 3D segmentation benchmark consists of 3D reconstructions of real rooms. The train set contains 1201 rooms. We split the ground truth segmentation masks for each object in all rooms resulting in 38349 scan-ground truth pairs for training.

ScanNetV2 validation set. The validation set of ScanNetV2 [7] contains 312 rooms. We create ground truth segmentation mask for each object in all rooms resulting in 10388 scan-ground truth pairs for testing.

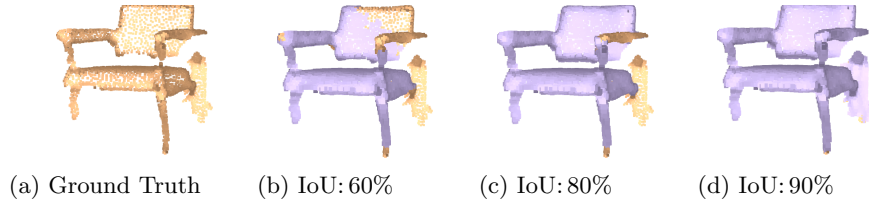


Fig. 4: Interactive object segmentation on images is evaluated on how many clicks are needed to reach a certain IoU between the predicted and ground-truth masks. Depending on the dataset the IoU needed to be reached is 80, 85 or 90. We believe that in order to get high quality segmentation masks, that can be used as ground truth, methods should focus on reaching approximately 90 % IoU. As it can be seen from the figures above a segmentation mask (purple) with 80% IoU still has significant erroneous regions.

S3DIS. The Stanford Large-Scale 3D Indoor Spaces (S3DIS) [1] dataset comprises of 3D scans of 6 large-scale indoor areas collected from 3 office buildings. The scans are represented as point clouds and are annotated with semantic labels of 13 object categories. Among the datasets used here for evaluation, S3DIS is probably the most similar one to ScanNet. We evaluate on the commonly used benchmark split (“Area 5 test”). It contains 240 scenes resulting in 2346 object instances for evaluating interactive object segmentation.

SemanticKITTI. SemanticKITTI [3] is a large-scale outdoor dataset. It shows traffic scenes recorded with a Velodyne-64 laser scanner. Its training set consists of 10 different driving sequences of total 9130 scenes. There are 28 annotated semantic classes from which 19 are evaluated. We evaluate scores in the single scan setting, i.e., individually per frame. We created 3609 scan-ground truth pairs based on sequence ‘01’ for evaluating interactive object segmentation. SemanticKITTI has the largest domain gap compared to our training set, as it contains outdoor traffic scenes with different point distributions and no color information.

Evaluation metrics. We perform the evaluation using the two standard metrics from the 2D domain [4, 16, 20, 22, 25, 33]: (1) **Number of Clicks (NOC)@q%**, the average number of clicks needed to reach q% Intersection over Union (IoU) between predicted and ground-truth masks on every object instance (thresholded at 20 clicks), and (2) **IoU@k**, the average IoU for k number of clicks per object instance.

4.2 Within-Domain Evaluation

At first, we evaluate our approach in training and testing on the same domain. In this scenario, we assume that we would like to extend an existing dataset by labeling more scenes. For this experiment, we use the ScanNetV2 dataset [7]. We use the official split of train-validation for our experiments. We fine-tune our

model on interactive object segmentation on the training subset of ScanNetV2 [7] and evaluate on the validation set. We unfortunately cannot evaluate on the test subset since no benchmark exists for interactive object segmentation and we require the instance masks to evaluate it by ourselves. ScanNetV2 [7] contains the segmentation masks for 40 classes. However, the ScanNetV2 [7] benchmark evaluates only on a 20-class subset (18 for instance segmentation). We used the 20-class subset of ScanNetV2 [7] training set to train our model, thus creating two subsets of the validation set: (1) *seen*, with object instances with classes of 20 object categories which have been seen in our training set and (2) *unseen*, with object instances with classes that have not been seen during training. The *seen* classes are also known as **ScanNetV2 Benchmark Classes** since these are the classes that are evaluated on the ScanNetV2 Benchmark.

Results. Results are summarized in Tables 1 and 2. There is no previous work that uses interactive object segmentation directly on the 3D domain therefore we evaluated our method on a 3D instance segmentation setup and compared our method with state-of-the-art fully supervised methods for 3D instance segmentation. As it can be seen, our method can offer segmentation masks of higher quality compared to instance segmentation methods with just a few clicks per object. With **5 clicks** per object it achieves **61.5 AP** compared to **55.1** of HAIS [5] and with **10 clicks** increases to **75.5 AP**.

The difference is more pronounced when we evaluate on the additional classes of ScanNetV2 [7]. ScanNetV2 [7] is a dataset with 40 labeled classes but most methods only evaluate on the 20-class subset. We trained our model only on the 20-class benchmark subset in contrast to HAIS [5] that trains on all classes. With just 2 additional clicks (Table 1, *bottom*) the AP can be doubled. You may see the improvement of the IoU per added click on Fig. 5 (*right*).

Our method is orthogonal to instance segmentation methods. We show that it can be used to improve the quality of segmentation masks at the cost of minimal user effort.

Our evaluation on the task of interactive object segmentation is presented in Table 2. To provide a frame of reference since there are no previous methods on interactive 3D object segmentation we report the scores (Table 2) from the first deep learning paper [33] on the task of 2D interactive object segmentation. Our scores are comparable with its 2D counterpart even though the 2D method uses pre-trained networks on much bigger datasets and some of the evaluation datasets contain only one object instance per image (eg., Grabcut) compared to the 30 objects of an average indoor 3D scene. The 2D method also employs an additional GraphCut refining.

We additionally report our scores compared to the method of Shen et al. [27] that segments objects using 2D scribbles. Shen et al. [27] report scores on selected classes of the Pix3D [29] dataset. Annotators labelled 95 randomly-selected objects to be used for fine-tuning a 3D reconstruction model pre-trained on synthetic data. Additionally it is not easy to define the size and form of the scribbles used and the labeled objects were un-occluded and un-truncated so

Table 1: **3D instance segmentation on ScanNetV2 validation set.** We evaluated our method on a 3D instance segmentation setup and compared it with state-of-the-art fully supervised methods for instance segmentation. For a fairer comparison we additionally evaluated HAIS [5] on a class agnostic setup where all predictions and ground truth belong to the same class *object*. Interactive object segmentation can offer better segmentation masks with a *few* user clicks per object. The difference is even more pronounced when we evaluate on the additional *unseen* classes of ScanNetV2. Segmentation masks are greatly improved with just 2 clicks per object even though our method is not trained on these additional classes.

	Method	AP	AP_50%	AP_25%
Benchmark Classes	SSTNet [21]	49.4	64.3	74.0
	HAIS [5]	43.5	64.1	75.6
	HAIS [5] class agnostic	55.1	75.3	84.9
	Ours (1 clicks per object)	20.9	38.0	67.2
	Ours (2 clicks per object)	37.9	60.8	84.3
	Ours (3 clicks per object)	48.1	73.4	90.7
	Ours (5 clicks per object)	61.8	86.0	95.7
	Ours (10 clicks per object)	75.5	94.8	99.0
	Ours (20 clicks per object)	80.3	96.6	99.3
Unseen Classes	HAIS [5] class agnostic	13.8	26.0	40.9
	Ours (1 clicks per object)	13.5	27.8	54.4
	Ours (2 clicks per object)	24.4	45.7	71.2
	Ours (3 clicks per object)	33.1	58.4	81.8
	Ours (5 clicks per object)	45.7	75.3	91.1
	Ours (10 clicks per object)	60.3	90.2	97.9
	Ours (20 clicks per object)	60.6	88.3	97.4

Table 2: **Within-Domain Evaluation.** Interactive 3D object segmentation results on ScanNetV2 validation set [7]. *Unseen* classes are not part of the training set. We report *Number of Clicks* (NOC)@80, 85 and 90 IoU. The lower the NOC value the better. For reference we provide the scores for the first deep learning method [33] for interactive 2D image segmentation. Some image datasets contain only a single object instance (eg. Grabcut) compared to the densely populated indoor point clouds (average ScanNetV2 scene contains 30 objects).

2D Domain	Pascal	Grabcut	Berkeley	MS COCO seen categories	MS COCO unseen categories
NOC @	85% IoU	90% IoU	90% IoU	85% IoU	85% IoU
DIOS with GC [33]	6.9	6.0	8.7	8.3	7.8
ScanNetV2 val - <i>Seen</i>				ScanNetV2 val - <i>Unseen</i>	
NOC @	80% IoU	85% IoU	90% IoU	80% IoU	85% IoU
Ours	08.3	10.6	13.6	11.6	14.1
				16.5	14.7

their statistics are not directly comparable with our evaluation on the densely populated datasets of ScanNetV2 validation and S3DIS but might show a trend for common object classes.

4.3 Out-of-Domain Evaluation.

In this section we evaluate the performance of our method on datasets different from our training dataset. We would like to see the performance of our model both in relatively small distribution shifts between training and test using two indoor datasets. (ScanNet \rightarrow S3DIS). Additionally we evaluate on large distribution shifts (ScanNet \rightarrow SemanticKITTI) by using our model trained on a indoor dataset and testing on an outdoor dataset containing very different objects and recorded with a different sensor like SemanticKITTI [3]. First, we use our model trained on ScanNetV2 train set **without any fine-tuning** on these datasets. We additionally report separate scores when online adaptation is used.

Results. Results are summarized in Tables 3 and 4. As it can be seen in Table 3-row 1) even though our interactive segmentation network was trained only on the ScanNet dataset it can still generalize easily on other indoor datasets like S3DIS. It even requires less clicks to achieve segmentation masks of the same quality. The more our test dataset distribution differs from the training the more clicks are required to achieve good segmentation mask as it can be seen from our results on semanticKITTI (Table 3). The semanticKITTI dataset requires more clicks for two reasons (1) its sparsity restricts the needed context from the click masks and (2) its characteristics (sparsity, no color, different sensor capturing the data) are very different from the training dataset. To that end, we incorporated an adaptation method that allows learning during test time from sparse user annotations [19]. As it can be seen (Table 3-row 2), that already helps significantly to adapt to new dataset distributions by require 4 less clicks. The adaptation does not help significantly on the S3DIS dataset since ScanNet and S3DIS do not differ as much as ScanNet and SemanticKITTI. However, if we look at the evaluation metrics per class (the method is class agnostic, we just aggregated the results per individual class), online adaptation helps significantly to segment object belonging to the classes of *board* and *beam* (Table 3). The two classes that do not exist in this form in the ScanNet dataset.

4.4 Qualitative Results.

We show visualizations of object segmentation on all three datasets in Fig. 10 and on full scenes Fig. 3. Our method predicts accurate and clear segmentations in

Table 3: **Out-of-Domain evaluation.** Interactive 3D object segmentation results on Stanford S3DIS [1] and SemanticKITTI [3] datasets. Training on ScanNetV2 generalizes well on S3DIS as both are indoor datasets containing similar objects. SemanticKITTI requires more clicks since it is probably the dataset most dissimilar to ScanNet. Online adaptation however bridges that gap.

NOC @	S3DIS Area 5			SemanticKITTI		
	80% IoU	85% IoU	90% IoU	80% IoU	85% IoU	90% IoU
Ours	6.8	8.9	11.8	19.4	19.5	19.6
Ours (on-line adaptation)	6.5	8.6	11.5	15.1	15.4	15.9

Table 4: **Per class interactive 3D object segmentation** on Stanford S3DIS [1] Area 5. Classes that are not part of the ScanNetV2 dataset like *beam* or not in the same form like *board* can benefit from online adaptation.

Method	NOC@90	Ceiling	Floor	Wall	Clutter	Column	Window	Door	Table	Chair	Bookcase	Sofa	Board	Beam
Ours	11.8	4.6	2.1	11.4	15.0	11.9	11.5	13.3	11.8	5.3	10.6	5.7	16.0	17.7
Ours - online adaptation	11.5	4.5	2.2	11.0	14.8	11.4	10.5	12.9	11.3	5.2	10.2	5.0	14.7	14.0

heavily cluttered environments with very few user clicks. Additional qualitative results are in the supplementary material.

4.5 Ablation on click mask size

We experimented with different length for *edge* (Sec. 3). *Edge* represents the size of the cube encoding the click mask. The best performing according to our experiments is $edge = 0.05m$. The cube representing the click contains approximately 30 points on the ScanNet dataset. This confirms the experiments of [4] where the best performing click mask in 2D is of radius=3. Please note we do not supervise the loss with the ground-truth of these points it is just the click encoding. For more details please see the supplementary material.

4.6 User Study


To evaluate our method with real human annotators, we also conducted a small scale experiment replacing the simulated annotator with three real human annotators in the loop. To that end, we implemented a interactive annotation tool that runs our model at the backend. The annotators engaged in the user study had no prior experience with annotating. We explained them how the tool works and allowed them to label a few examples to familiarize themselves with the tool before recording their behavior. The annotators see the full scene as does the simulated annotator without cropping or using bounding boxes. They could submit their segmentation as final at anytime if they were satisfied with the segmentation.

First we asked the annotators to label 10 random objects from the challenging class *picture* using our interactive segmentation tool and we compared the real

Table 5: **3D clicks compared to 2D scribbles**. [27] annotated a few example objects on Pix3D [29] to train networks for 3D reconstruction. Their statistics are not directly comparable to ours since they are performed on a different dataset (with un-occluded objects) using 2D scribbles instead of 3D points but it offers some understanding on the task.

	Annotations	Dataset	Bed	Bookcase	Desk	Sofa	Table	Wardrobe
SIM [27]	2D scribbles	Pix3D	15	18	10	10	19	9
Ours	3D clicks	S3DIS	-	10.6	-	5.7	11.8	-
Ours	3D clicks	ScanNetV2 val.	16.3	15.7	18.5	12.5	11.8	-

Table 6: **Real Human Annotators User Study.** Real human annotators were asked to label points of the class *picture* (*table*, *left*) and a set of random objects (*table*, *right*). Real human annotators performed actually slightly better when asked to label the challenging class *picture* than the simulated clicks especially in the low clicks regime. This shows that our simulation strategy is representative of real human input and produces similar results.

	ScanNetV2- <i>picture</i>		ScanNetV2- <i>random</i>		
	IoU@5	IoU@10	IoU@5	IoU@10	
Human	49.6	57.0	78.1	82.0	
Simulator	32.0	54.5	79.8	84.8	

users results with the corresponding results from the simulated annotator (*Task 1*). Then we asked the annotators to randomly segment 20 objects from ScanNetV2 validation set and compared them with the same objects annotated by the simulated annotator (*Task 2*). The results are presented in Table 6. Task 1 is especially challenging as it can be seen from the example figure of our user interface (right). The geometry of the points belonging to the class is very similar to the geometry of the wall nearby and only color can help distinguish the separate objects. Despite that, real human annotators performed actually slightly better than the simulated clicks especially in the low clicks regime. Labeling random objects also performs similarly to the simulated clicks.

We note that although our model is trained with simulated clicks, it can show robustness to human input even though they follow different labelling strategies and that our simulation of interactive object segmentation (Sec. 3) is representative of real human input and both provide similar output.

5 Limitations and Future Work

Our approach is the first attempt to establish a state-of-the-art for interactive object segmentation in 3D point clouds. As promising future directions, we envi-

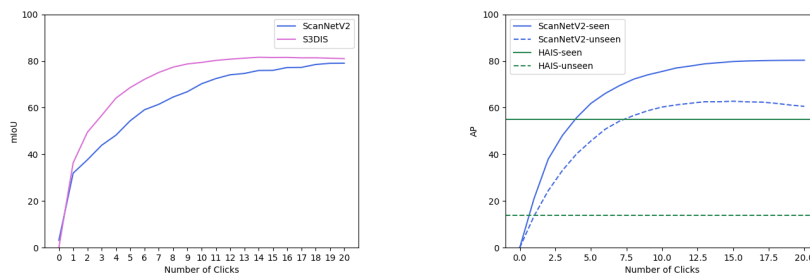


Fig. 5: (Left:) **Mean IoU@k** for varying clicks k on ScanNetV2 [7] and S3DIS [1] dataset. (Right:) **AP** for varying clicks k on the ScanNetV2 *seen* and *unseen* classes compared to state-of-the-art 3D instance segmentation method of HAIS [5].

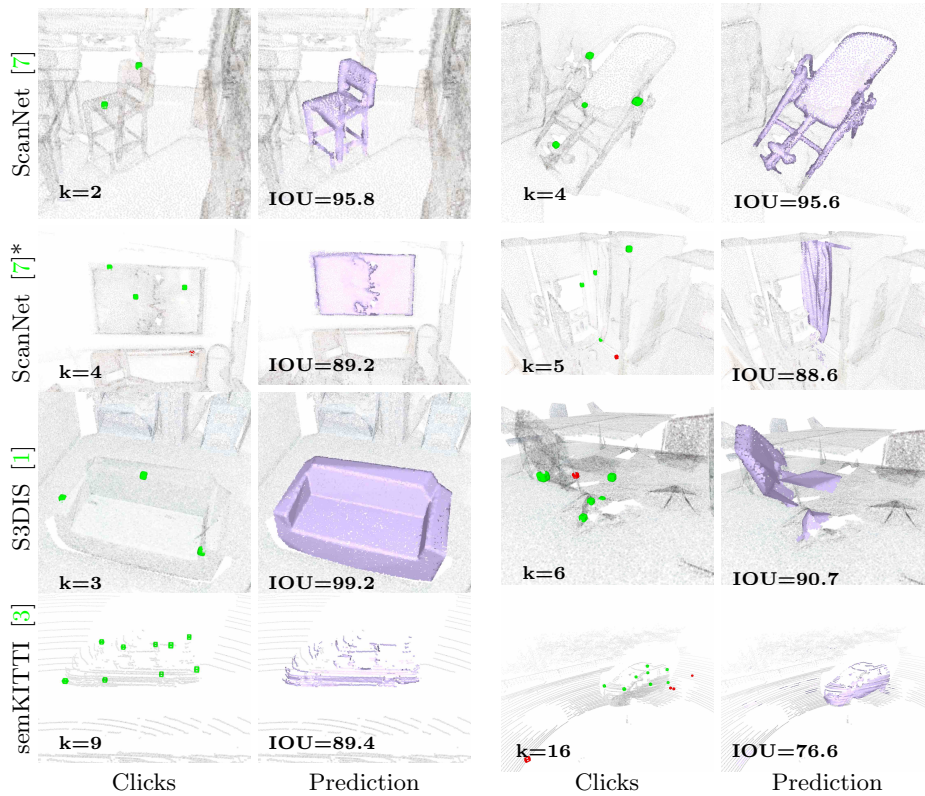


Fig. 6: **Qualitative results** with clicks and corresponding segmentation masks. Our approach accurately segments objects from different datasets with as few as two user clicks (*top row, left*). ScanNet* (*second row*) shows examples of classes not part of the ScanNet training set: *television (left)* and *shower curtain (right)*.

sion several ways to further improve the segmentation outcome of the interactive model: (1) enhancing the input with pre-trained semantic and instance backbones (2) incorporating the output segmentation masks from previous user interactions as additional input for the next correction (3) use of the iterative sampling strategy [25] to emulate a real user interaction during training (4) different loss strategies that deal with class imbalance between foreground and background.

6 Conclusion

In this work, we have introduced a first state-of-the-art for interactive segmentation of 3D objects based purely on 3D interaction between the user and a point cloud. It is a simple but yet powerful framework that shows we can achieve accurate 3D segmentation masks with little human effort, generalises well to different datasets and can lead to the easier creation of realistic large-scale 3D training sets. We presented a practical policy for simulating user clicks for easy and accurate evaluation, along with a small user study that verified its validity.

References

1. Armeni, I., Sener, O., Zamir, A.R., Jiang, H., Brilakis, I., Fischer, M., Savarese, S.: 3D Semantic Parsing of Large-Scale Indoor Spaces. In: Proceedings of the IEEE Conference on Computer Vision and Pattern Recognition (2016) [2](#), [7](#), [8](#), [11](#), [12](#), [13](#), [14](#), [21](#)
2. Baruch, G., Chen, Z., Dehghan, A., Dimry, T., Feigin, Y., Fu, P., Gebauer, T., Joffe, B., Kurz, D., Schwartz, A., Shulman, E.: Arkitscenes - a diverse real-world dataset for 3d indoor scene understanding using mobile rgb-d data (2021), <https://arxiv.org/pdf/2111.08897.pdf> [18](#), [20](#)
3. Behley, J., Garbade, M., Milioto, A., Quenzel, J., Behnke, S., Stachniss, C., Gall, J.: SemanticKITTI: A Dataset for Semantic Scene Understanding of LiDAR Sequences. In: Proceedings of the International Conference on Computer Vision (2019) [6](#), [7](#), [8](#), [11](#), [14](#), [21](#)
4. Benenson, R., Popov, S., Ferrari, V.: Large-scale interactive object segmentation with human annotators. In: Proceedings of the IEEE Conference on Computer Vision and Pattern Recognition (2019) [1](#), [2](#), [5](#), [8](#), [12](#)
5. Chen, S., Fang, J., Zhang, Q., Liu, W., Wang, X.: Hierarchical aggregation for 3d instance segmentation. In: ICCV (2021) [4](#), [9](#), [10](#), [13](#)
6. Choy, C., Gwak, J., Savarese, S.: 4D Spatio-Temporal ConvNets: Minkowski Convolutional Neural Networks. In: Proceedings of the IEEE Conference on Computer Vision and Pattern Recognition (2019) [3](#), [6](#)
7. Dai, A., Chang, A.X., Savva, M., Halber, M., Funkhouser, T., Nießner, M.: ScanNet: Richly-annotated 3d reconstructions of indoor scenes. In: Proceedings of the IEEE Conference on Computer Vision and Pattern Recognition (2017) [2](#), [3](#), [6](#), [7](#), [8](#), [9](#), [10](#), [13](#), [14](#), [18](#), [19](#), [21](#)
8. Deng, J., Dong, W., Socher, R., Li, L.J., Li, K., Fei-fei, L.: ImageNet: A large-scale hierarchical image database. In: Proceedings of the IEEE Conference on Computer Vision and Pattern Recognition (2009) [7](#)
9. Engelmann, F., Bokeloh, M., Fathi, A., Leibe, B., Nießner, M.: 3D-MPA: Multi Proposal Aggregation for 3D Semantic Instance Segmentation. In: Proceedings of the IEEE Conference on Computer Vision and Pattern Recognition (2020) [4](#)
10. Everingham, M., Van Gool, L., Williams, C.K.I., Winn, J., Zisserman, A.: The PASCAL Visual Object Classes Challenge 2012 (VOC2012) Results. <http://www.pascal-network.org/challenges/VOC/voc2012/workshop/index.html> (2012) [7](#)
11. Graham, B., Engelcke, M., van der Maaten, L.: 3D Semantic Segmentation with Submanifold Sparse Convolutional Networks. In: Proceedings of the IEEE Conference on Computer Vision and Pattern Recognition (2018) [6](#)
12. He, K., Gkioxari, G., Dollár, P., Girshick, R.: Mask r-cnn. In: Proceedings of the International Conference on Computer Vision [4](#)
13. Hou, J., Dai, A., Nießner, M.: 3D-SIS: 3D Semantic Instance Segmentation of RGB-D Scans. In: Proceedings of the IEEE Conference on Computer Vision and Pattern Recognition (2019) [4](#)
14. Hou, J., Graham, B., Nießner, M., Xie, S.: Exploring data-efficient 3d scene understanding with contrastive scene contexts. In: Proceedings of the IEEE/CVF Conference on Computer Vision and Pattern Recognition. pp. 15587–15597 (2021) [2](#), [4](#)
15. Hou, J., Graham, B., Nießner, M., Xie, S.: Exploring data-efficient 3d scene understanding with contrastive scene contexts. In: Proceedings of the IEEE/CVF Conference on Computer Vision and Pattern Recognition. pp. 15587–15597 (2021) [4](#)

16. Jang, W.D., Kim, C.S.: Interactive image segmentation via backpropagating refinement scheme. In: Proceedings of the IEEE Conference on Computer Vision and Pattern Recognition (2019) [2](#), [6](#), [8](#)
17. Jiang, L., Shi, S., Tian, Z., Lai, X., Liu, S., Fu, C.W., Jia, J.: Guided point contrastive learning for semi-supervised point cloud semantic segmentation. In: Proceedings of the IEEE/CVF International Conference on Computer Vision. pp. 6423–6432 (2021) [2](#), [4](#)
18. Jiang, L., Zhao, H., Shi, S., Liu, S., Fu, C.W., Jia, J.: PointGroup: Dual-set Point Grouping for 3D Instance Segmentation. In: Proceedings of the IEEE Conference on Computer Vision and Pattern Recognition (2020) [4](#)
19. Kontogianni, T., Gygli, M., Uijlings, J., Ferrari, V.: Continuous Adaptation for Interactive Object Segmentation by Learning from Corrections. In: Proceedings of the European Conference on Computer Vision (2020) [6](#), [11](#)
20. Li, Z., Chen, Q., Koltun, V.: Interactive image segmentation with latent diversity. In: Proceedings of the IEEE Conference on Computer Vision and Pattern Recognition (2018) [2](#), [6](#), [8](#)
21. Liang, Z., Li, Z., Xu, S., Tan, M., Jia, K.: Instance segmentation in 3d scenes using semantic superpoint tree networks. In: Proceedings of the IEEE/CVF International Conference on Computer Vision. pp. 2783–2792 (2021) [4](#), [10](#)
22. Liew, J., Wei, Y., Xiong, W., Ong, S.H., Feng, J.: Regional interactive image segmentation networks. In: Proceedings of the International Conference on Computer Vision (2017) [2](#), [6](#), [8](#)
23. Lin, T.Y., Maire, M., Belongie, S., Hays, J., Perona, P., Ramanan, D., Dollár, P., Zitnick, C.: Microsoft COCO: Common objects in context. In: Proceedings of the European Conference on Computer Vision (2014) [7](#)
24. Liu, Z., Qi, X., Fu, C.W.: One thing one click: A self-training approach for weakly supervised 3d semantic segmentation. In: Proceedings of the IEEE/CVF Conference on Computer Vision and Pattern Recognition. pp. 1726–1736 (2021) [2](#), [4](#)
25. Mahadevan, S., Voigtlaender, P., Leibe, B.: Iteratively trained interactive segmentation. In: Proceedings of the British Machine Vision Conference (2018) [2](#), [6](#), [7](#), [8](#), [14](#)
26. Qi, C.R., Yi, L., Su, H., Guibas, L.J.: PointNet++: Deep Hierarchical Feature Learning on Point Sets in a Metric Space. In: Advances in Neural Information Processing Systems (2017) [3](#)
27. Shen, T., Gao, J., Kar, A., Fidler, S.: Interactive Annotation of 3D Object Geometry using 2D Scribbles. In: Proceedings of the European Conference on Computer Vision (2020) [2](#), [3](#), [4](#), [9](#), [12](#)
28. Sofiiuk, K., Petrov, I.A., Konushin, A.: Reviving iterative training with mask guidance for interactive segmentation. arXiv preprint arXiv:2102.06583 (2021) [5](#)
29. Sun, X., Wu, J., Zhang, X., Zhang, Z., Zhang, C., Xue, T., Tenenbaum, J.B., Freeman, W.T.: Pix3D: Dataset and Methods for Single-Image 3D Shape Modeling. In: IEEE Conference on Computer Vision and Pattern Recognition (CVPR) (2018) [9](#), [12](#)
30. Thomas, H., Qi, C.R., Deschaud, J.E., Marcotegui, B., Goulette, F., Guibas, L.J.: KPConv: Flexible and Deformable Convolution for Point Clouds. In: Proceedings of the International Conference on Computer Vision (2019) [3](#)
31. Wang, H., Rong, X., Yang, L., Feng, J., Xiao, J., Tian, Y.: Weakly supervised semantic segmentation in 3d graph-structured point clouds of wild scenes. arXiv preprint arXiv:2004.12498 (2020) [2](#), [4](#)

32. Wang, X., Liu, S., Shen, X., Shen, C., Jia, J.: Associatively Segmenting Instances and Semantics in Point Clouds. In: Proceedings of the IEEE Conference on Computer Vision and Pattern Recognition (2019) [4](#)
33. Xu, N., Price, B., Cohen, S., Yang, J., Huang, T.: Deep interactive object selection. In: Proceedings of the IEEE Conference on Computer Vision and Pattern Recognition (2016) [2](#), [6](#), [8](#), [9](#), [10](#)
34. Xu, X., Lee, G.H.: Weakly supervised semantic point cloud segmentation: Towards 10x fewer labels. In: Proceedings of the IEEE/CVF conference on computer vision and pattern recognition. pp. 13706–13715 (2020) [2](#), [4](#)
35. Yang, B., Wang, J., Clark, R., Hu, Q., Wang, S., Markham, A., Trigoni, N.: Learning Object Bounding Boxes for 3D Instance Segmentation on Point Clouds. In: Advances in Neural Information Processing Systems (2019) [4](#)
36. Zhang, Y., Qu, Y., Xie, Y., Li, Z., Zheng, S., Li, C.: Perturbed self-distillation: Weakly supervised large-scale point cloud semantic segmentation. In: Proceedings of the IEEE/CVF International Conference on Computer Vision. pp. 15520–15528 (2021) [2](#), [4](#)
37. Zhi, S., Sucar, E., Mouton, A., Haughton, I., Laidlow, T., Davison, A.J.: iLabel: Interactive Neural Scene Labelling. arXiv (2021) [2](#)

A Overview

In Fig. 7 we show an overview of the interactive 3D object segmentation pipeline.

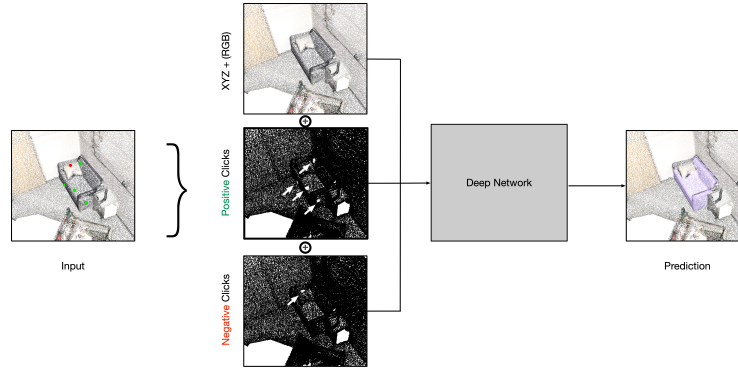


Fig. 7: **Overview of the method.** The input consists of a point cloud with two additional channels concatenated, one for the positive and one for the negative clicks. (*The arrows in the positive and negative click channels are drawn to help the viewer spot the corresponding clicks masks easier in 3D.*)

B Correcting Existing Ground Truth

We have labeled objects from the ScanNetV2 [7] from scratch. We noticed discrepancies in the ground truth provided already with the ScanNet dataset as it can be seen in Fig. 8. One can use interactive object segmentation to refine the given ground truth on existing datasets and thus provide the community with improved labeled data.

C Labeling New Datasets

ARKitScenes [2] is a new diverse 3D Indoor Scene dataset. The ground truth provided is only in the form of bounding boxes around the 3D objects. We used our interactive object annotation method to label objects from the test dataset and thus enhancing the dataset with accurate segmentation masks. As it can be seen in the supplementary video our method, trained on ScanNet can be used on a different dataset on classes that have never been seen during training (eg. Christmas Tree).



Fig. 8: **Refining existing ground truth on ScanNetV2.** Labeling datasets is a difficult task. There often times that even the ground truth data is not very accurate. We tested our interactive object segmentation method using our simple labeling tool and we could correct mistakes in the ground truth of existing labeled datasets.

D Implementation Details

We train our network on the task of interactive 3D object segmentation with Adam optimizer using a learning rate of 0.001 with batch size of 10. We use cropped scenes of $5 \times 5 \text{ m}^2$ during training but we test on full scenes.

E Click Mask Size

We tested different *edge* lengths for the cubic click mask (Eq. 1 in main paper). The best performing is 5 cm as it can be seen in Table 7. We experimented on using different size of click masks between train and test and the result is still robust with a small penalty in the number of clicks (Table 7, row 3). In all our experiments in the main paper we use the length of 5 cm.

Table 7: **Size of click mask.** Best length for the clicks mask is 5 cm. A cube of edge length of 5 cm contains approximately 30 points on average on the ScanNetV2 [7] dataset.

ScanNetV2 val	NOC@90
5cm \rightarrow 5cm	14.72
10cm \rightarrow 10cm	16.09
5cm \rightarrow 10cm	15.88



Fig. 9: **Labeling New Dataset.** We tested our method on labeling objects from the ARKitScenes [2] dataset. ARKitScenes does not contain segmentation masks only bounding boxes. The scenes are challenging with a lot of clutter. We labeled objects of classes existing in the train set (eg. sofa) but also classes that have never been seen during training (eg. bottle).

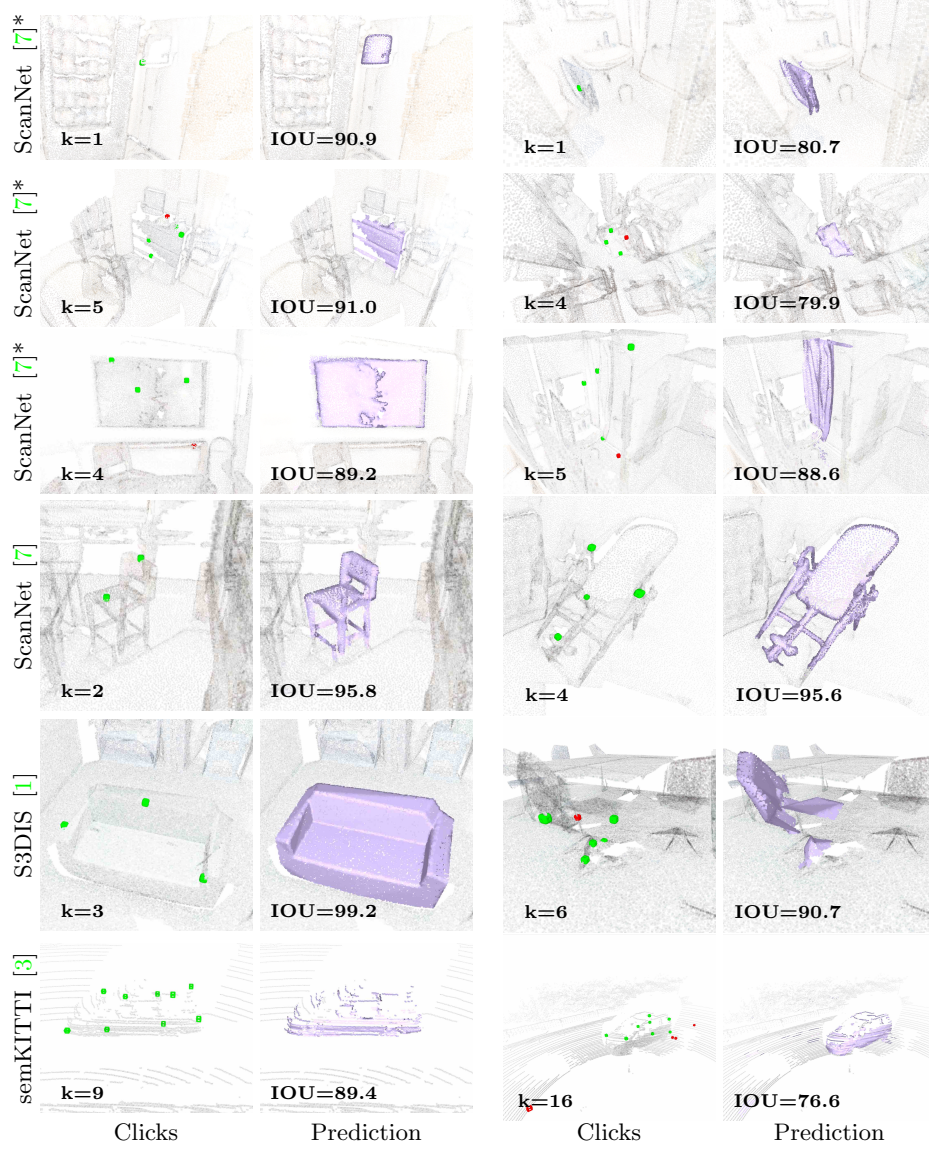


Fig. 10: **Additional qualitative results** with clicks and corresponding segmentation masks. Our approach accurately segments objects from different datasets. ScanNet* shows examples of classes not part of the ScanNet training set such as *towel*, *pillow*, *lamp*, *television* and *shower curtain*. The method is capable of segmenting challenging objects like *towel* and *shower curtain* with a few clicks.